Synthesis and Characterization of Nano Au/NPAA Templates

Mohamed Shaban

Nanophononics and Applications Labs, Department of Physics, Faculty of Science, Beni-Suef University, Egypt

Department of Physics, Faculty of Science, Islamic University of Madinah, KSA

mssfadel@aucegypt.edu

and

Sobhi M. Gomha

Department of Chemistry, Faculty of Science, Cairo University, Egypt.

Department of Chemistry, Faculty of Science, Islamic University of Madinah, KSA

s.m.gomha@gmail.com

Abstract: A modified two-step anodization process was applied for preparing highly ordered nanoporous anodic alumina (NPAA) templates. The interpore distance and the diameter of the NPAA pores were, 100 nm and 80 ± 2 nm, respectively. Then, Au sputtering was carried out over the fabricated template using r.f. magnetron sputtering. The morphological characterization showed that hexagonal Au nanoarrays have been deposited on the top surface of the NPAA template. Simultaneously, the interior walls of the NPAA pores have been decorated with fine Au nanoparticles. The Au-coated samples showed brilliant and statured structural colors due to the surface plasmon resonance (SPR) enhancement of NPAA optical interference. The SPR wavelength is increased from 466 nm to 512 nm by increasing the Au deposition time from 1 to 2 min.

Keywords: Nanoporous membranes; Au nanostructures; Surface plasmon resonance; r.f. magnetron sputtering

توليف وتوصيف قوالب Nano Au / NPAA

الملخص: تم تطبيق عملية أنودة معدلة من خطوتين لإعداد قوالب أنوديك ألومينا نانوية (NPAA) عالية الترتيب. حيث كانت المسافة البينية وقطر مسام ال NPAA، ١٠٠ نانومتر و٨٠ ± ٢ نانومتر، على التوالي. بعد ذلك، تم ترسيب جسيمات الذهب النانوية على سطح القالب المصطنع باستخدام طريقة (r.f. sputtering). أظهر التوصيف المورفولوجي أن مصفوفات نانوية سداسية الترتيب من جسيمات الذهب النانوية قد ترسبت على السطح العلوي للقالب. في الوقت نفسه، تم تزيين الجدران الداخلية لمسام ال NPAA بجسيمات الذهب النانوية الدقيقة. أظهرت العينات المطلية بـجسيمات الذهب ألوانًا هيكلية رائعة وثابتة نظرًا لتعزيز رنين البلازمون السطحي SPR مع التداخل البصري لـ NPAA كما لوحظ زيادة الطول الموجي ل SPR من ٤٦٦ نانومتر إلى ٥١٢ نانومتر بزيادة وقت ترسيب الذهب من ١ إلى ٢ دقيقة.

1. Introduction

During the recent decade, great efforts have been directed toward the design and characterization of the nanoporous templates because of their wide range of applications [1-4]. Nanoporous anodic alumina (NPAA) is an interesting porous template with a bright color in the visible light range due to the interference of light [1]. The saturation of the color is very low. To get a highly saturated color and to extend the applications of NPAA, plasmonic nanostructures were applied to coat the nanopores of the NPAA [1, 5].

Gold (Au) is one of the most important plasmonics nanomaterials. The design and optical characterization of Au nanostructures have been extensively addressed [6-9]. The existence of the localized surface plasmon resonances is considered one of the most important features that make Au nanostructures a key material in many applications. The positions of the localized surface resonances are size- and shape-dependent. Also, the surface plasmon resonance coupling shifts the resonance wavelength and splits the degenerated modes for regular Au nanoarrays. So Au nanoarrays can be applied for guiding, enhancing, emitting, and modifying the optical response for different applications including nanoplasmonic-photonic crystals[10], surface-enhanced Raman scattering (SERS)-based sensors [11], and nanoctylasts[12]. Consequently, the controllable deposition of Au nanoarrays on NPAA templates to produce Au/NPAA nanoporous structures is required to address the coupling between surface plasmon of Au nanoarrays and NPAA interference.

To deposit Au nanoarrays on the top surface of NPAA, a deposition technique such as radio frequency (r.f.) magnetron sputtering was applied because it permits the accurate controller of size, shape, and the composition. But, Au nanoparticles are also deposited on the interior walls of the pores of the NPAA template during the deposition process. Therefore, the full optical characterization of the Au/NPAA nanoporous arrays is complicated because of the existence of more than one Au nanoarray, Al substrate, and the electromagnetic coupling among the closest Au nanoparticles. Based on the previous reasons it is imperative to study the design of Au/NPAA nanoarrays experimentally and to correlate between the SPR positions and the morphological parameters of Au nanoarrays.

In this article, a modified two-step anodization process was applied to design NPAA templates. Then, the simultaneous decoration of the interior wall of NPAA nanopores and the growth of Au nanoarrays on the top surface of the NPAA template was performed by r.f. magnetron sputtering. Then, the morphological properties of NPAA and Au/NPAA are studied using field emission scanning electron microscope (SEM). Also, the optical properties are

studied using UV/Vis/NIR spectrophotometer. Moreover, the role of localized and propagating surface plasmons (LSP and PSP) on the enhancement of optical interference between the light beams reflected from the top and bottom surface of Au/PAA film was discussed.

2. Experiments: Fabrication and Characterization

Al foil with purity 99.99% has been used as a starting material for the fabrication of nanoporous anodic alumina (NPAA) template. Frist The Al foil (99.99%) was electropolished using a mixture of H_3PO_4 and H_2SO_4. The electropolished Al foil was anodized in 0.3 M oxalic acid at 40 V for 2 h. After removing the alumina layer, the 2nd anodization was carried for 5 min under the conditions and followed by the barrier-thinning process by a successive drop of the DC voltage at a rate of 0.1 V/s [13-15]. The pores of the NPAA were widened by immersing the NPAA into 6 wt% H_3PO_4 for 70 min. Au sputtering was carried out on the NPAA templates by r.f. magnetron sputtering at 65W for 1 and 2 min. The target-substrate distance was fixed at 100 mm. The Ar gas pressure was fixed at 5 mTorr during the deposition at room temperature.

The morphological parameters are characterized by field emission scanning electron microscopy (FE-SEM, JSM-7500F/JEOL). The optical properties of the uncoated and coated membranes were characterized using UV-Vis-NIR Perkin Elmer (Lambda 990) spectrophotometer.

3. Results and discussion

3.1 General NPAA morphological Properties

The topographical and morphological properties of the blank NPAA template were characterized through the FESEM images. Figure 1 shows FESEM images of NPAA template anodized for 5 min and pore widened for 70 min; (a) a cross-sectional FESEM and (b) top view FESEM. Figure 1(a) clearly shows the fabrication of highly ordered and homogenous circular nanopores in regular hexagonal nanoarrays. The diameter of the circular pores is 80 ± 2 nm. The average value of the distance between the pores, interpore distance, is ~ 100 nm. The density of the pores was estimated to be ~ 1.2×10^{10} cm^{-2}. The cross-sectional FESEM, Fig.1(b), shows smooth pores with a circular cross-section. The height of pores from the Al substrate is 410.9±8 nm. This means that the rate of growth of the alumina pores was 82.18±1.6 nm/min. The EDX spectrum of the NPAA membrane is shown in the inset of Figure 1(a). Only Al and O signals are observed, which confirm the high purity of the prepared NPAA membrane.

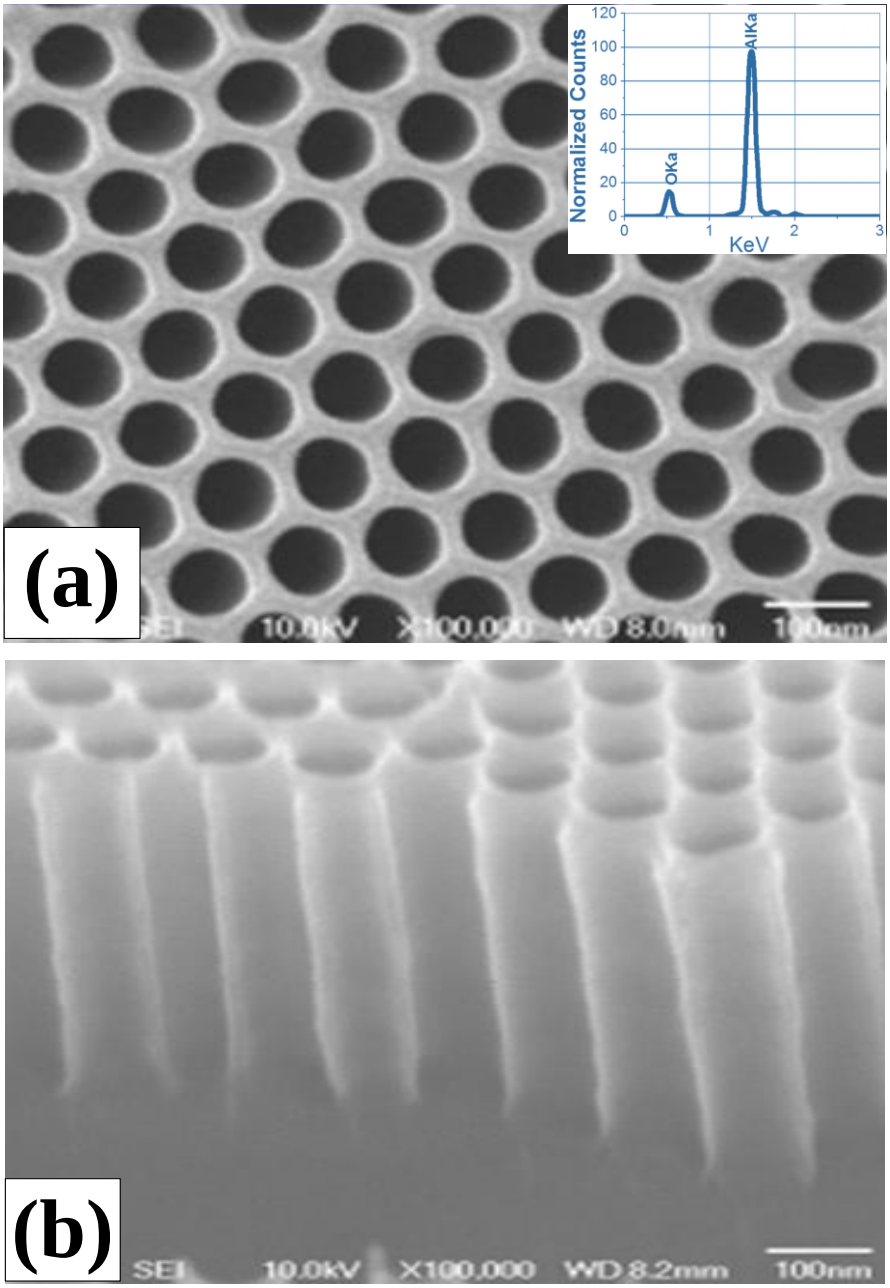

Figure 1. FESEM images of NPAA template fabricated using a two-step anodization process with 5 min second anodization followed by a 70 min pore widening process (a) top view and (b) cross-sectional view.

3.2 Morphological properties of Au/NPAA template

Figure 2 shows the FESEM image of the NPAA membrane sputtered with Au for 2 min. This image shows the growth of hexagonal nanoarray of six Au nanoparticles around each pore of the NPAA template. The narrow gap between each two successive Au particles is varied up to ~ 24 nm. Of course, the control of the Au particle size and the distance between the successive particles is sputtering time-dependent. As the sputtering time decreased, the Au nanoparticle size decreased and the gaps between the particles increased. The average Au deposition rate is

~ 14.7 nm/min. Also, the NPAA pore diameter is decreased due to the growth of Au nanoparticles on the surfaces of pore walls as seen from the inset image of Fig.2. The size distribution of these Au nanoparticles is very narrow and the density of these Au nanoparticles is very high. Generally, Au nanoparticles are grown perpendicularly on the NPAA substrate with a pronounced homogeneity in their size, shape, and density. The improved morphological properties of the Au nanoarrays could be ascribed to the homogeneity and quality of the used NPAA as a template for the deposition of plasmonic nanoarrays as discussed previously in the literature [16]. So, it is highly expected that the designed Au/NPAA can be used for different applications including catalytic systems, imaging- and diagnostic-based applications, and sensors. Hence we motivated to study the optical properties of NPAA and Au/NPAA templates.

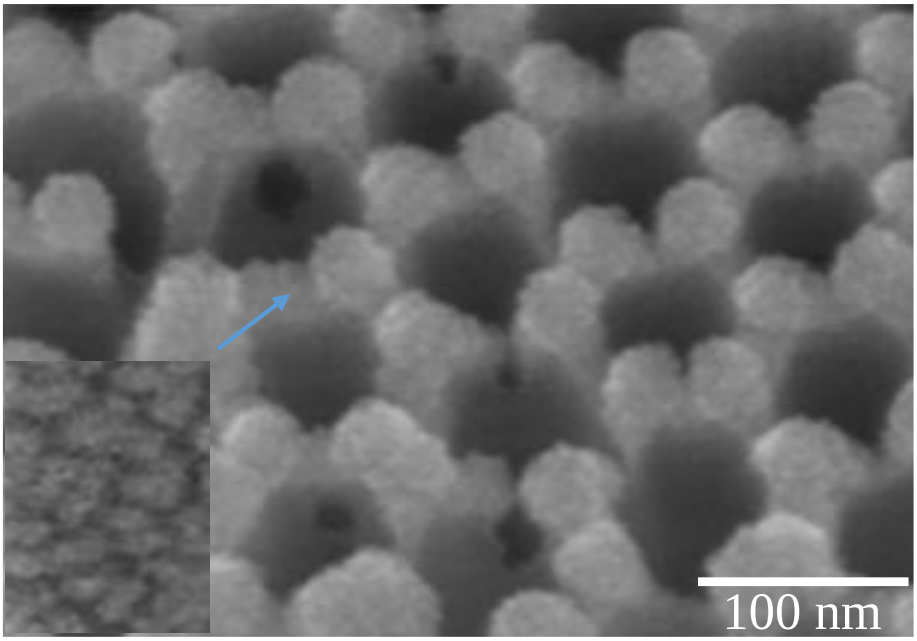

Figure 2. FESEM image NPAA template sputtered with Au for 2 min. The inset shows an enlarged FESEM image for Au nanoparticles on the pore wall.

3.3 Optical properties of NPAA and Au/NPAA templates

Figure 3 shows the reflectance spectra of uncoated and Au-coated NPAA templates for 1 min and 2 min. The reflectance spectra were measured within the spectral range 400-1000 nm using UV-Vis-NIR Perkin Elmer (Lambda 990) spectrophotometer. The main observed feature in the measured spectra indicates the interference between the reflected rays from Al/NPAA, NPAA/Au, and Au/air interfaces. So, well-set crests and troughs are observed. However, many other interesting features can be observed over the investigated spectral range. First, The reflectivity of the Au/NPAA templates is lower than the reflectivity of the uncoated NPAA template and change smoothly over the studied spectral range. Second, the reflectivity of the 1

min Au coated sample is blue-shifted and as the sputtering time increased the reflectivity increased and the reflection spectrum is redshifted. Thirdly, the saturation and the strength of the interference fringes of the Au-coated NPAA templates are highly improved relative to that of the blank NPAA.

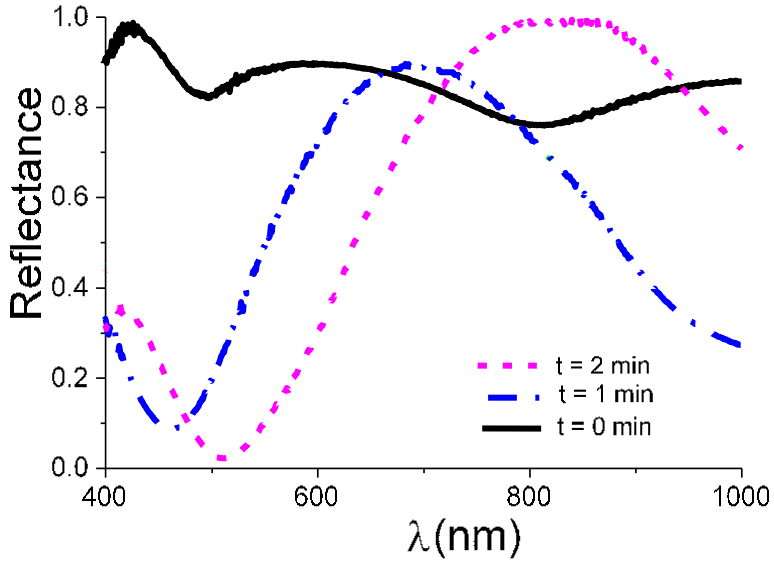

Figure 3. Reflectance spectra of uncoated, 1 min Au-coated, and 2 min Au-coated NPAA templates.

A potential explanation behind this behavior is proposed as follows. Figure 4(A) shows a schematic chart of the surface plasmon resonances coupling that produced between closest nanoparticles. This coupling causes much stronger surface plasmon resonance (SPR) modes as mentioned in literature [17, 18]. Figure 4(B) shows a schematic diagram of the deposited Au nanoarrays around each pore and on the inside pore walls. This figure also shows the generated surface SPR modes from Au/NPAA interfaces. The created surface plasmon at the Au/NPAA interface can go about as another exciting source because it can propagate into the Al_2O_3 and Al layers [19]. Here, the Au nanoarrays possess narrow gaps < 24 nm, so strong coupling, and intense SPR can be generated. For whatever length of time that the Au nanoparticles of the nanoarray come up short on a direct conductive interlink, their closeness creates negative dipole-dipole coupling energy that leads to the SPR redshift [20]. This redshift depends upon the Au particle size and the gap between the Au nanoparticles. At 1 min Au coating, the SPR wavelength is centered at 466 nm and shifted to 512 nm by expanding the deposition time to 2 min (jump 46 nm). Also, the wavelength at the maximum reflectance (λmax) is increased from about 700 to 850 nm by increasing the Au deposition time from 1 to 2 min. Thus, enormous optical fields are amassed in the leading connections between the particles of the nanoarray. Our data agree well with the previously reported data in the literature [20-22] that anomalous

enhancement impacts due to SPR and coupling can happen between the contacting surfaces of Au nanoarrays. As shown in Fig.4 (C, D), the Au coated NPAA templates showed brilliant colors with amazing saturation due to the SPR enhancement of optical interference. The photographs showed brilliant structural colors due to the strong light mirroring at certain wavelengths. As shown the colors of the samples are mostly depending on the coating time and changed from red to brown as the time increased from 1 to 2 min.

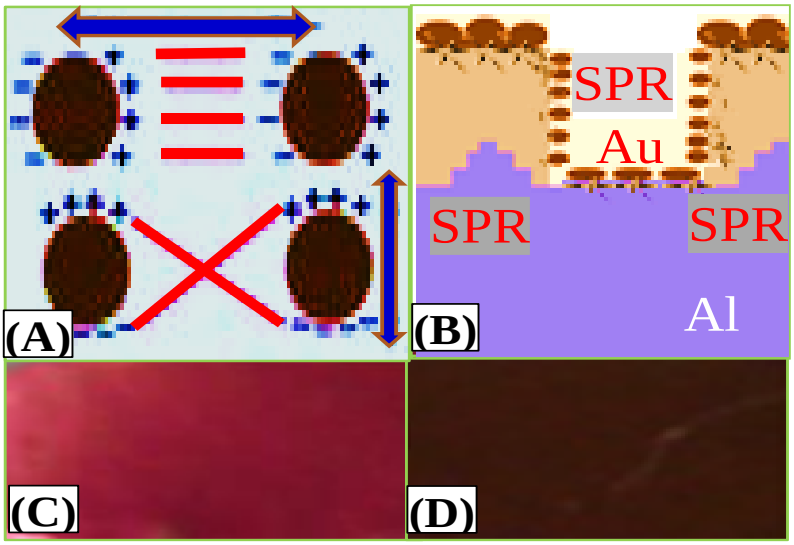

Figure 4. (A) Schematic diagram of SPR coupling modes, (B) SPR modes of Au/NPAA template, and Photographic images of (C) 1 min Au/NPAA and (D) 2 min Au/NPAA.

4. Conclusion

NPAA templates with 100 nm inter-pore distance have been fabricated by modified two-step anodization. Hexagonal Au nanoarrays have been deposited on the top surface of the NPAA template using r.f. magnetron sputtering. Simultaneously, the interior surfaces (walls) of the pores have been decorated with fine Au nanoparticles. The Au-coated templates showed brilliant and statured structural colors due to the SPR enhancement of NPAA optical interference. The SPR wavelength is increased from 466 nm to 512 nm by increasing the Au deposition time from 1 to 2 min. Because the used technique for the design of these nanostructures is simple, fast, inexpensive, and reproducible, therefore, the designed Au/NPAA nanoarrays can serve as key materials for nanophotonic and nanoelectronics devices.

5. References

[1] J. W. Diggle, T. C. Downie, and C.W. Goulding. Anodic oxide films on aluminum. Chem. Rev. 69 (1969) 365-405.

[2] Y. Yamamoto, N. Baha, and S. Tajima. Coloured materials and photoluminescence centres in anodic film on aluminium. Nature 289 (1981) 572-574.
[3] Y. Du, W.L. Cai, C.M. Mo, J. Chen, L.D. Zhang and X.G. Zhu. Preparation and photoluminescence of alumina membranes with ordered pore arrays. Appl. Phys. Lett. 74 (1999) 2951
[4] G. Wang, C. –W. Wang, Y. Li, W. –M. Liu, Thin Solid Films 516 (2008) 6789 -6798.
[5] X. H. Wang, T. Akahane, H. Orikasa, T. Kyotani, and Y. Y. Fu. Brilliant and tunable color of carbon-coated thin anodic aluminum oxide films. Appl. Phys. Lett. 91(2007) 011908.
[6] C. Hsu, and H. H. Liu, Optical behaviours of two dimensional Au nanoparticle arrays within porous anodic alumina. Journal of Physics: Conference Series. 61 (2007) 440-444
[7] S. L. Pan, D. D. Zeng, H. L. Zhang, H. L. Li. Preparation of ordered array of nanoscopic gold rods by template method and its optical properties. Appl. Phys. A 70 (2000) 637-640.
[8] K. L. Kelly, E. Coronado, L. L. Zhao, and G.C. Schatz. The Optical Properties of Metal Nanoparticles: The Influence of Size, Shape, and Dielectric Environment. J. Phys. Chem. B 107 (2003) 668-677.
[9] G. A. Wurtz, W. Dickson, D. O'Connor, R. Atkinson, W. Hendren, P. Evans, R. Pollard, and A.V. Zayats. Guided plasmonic modes in nanorod assemblies: strong electromagnetic coupling regime. Optics Express 16 (2008) 7460-7470.
[10] X. Zhang, B. Sun, H. Guo, N. Tetreault, G. Giessen, R. H. Friend. Large-area two-dimensional photonic crystals of metallic nanocylinders based on colloidal gold nanoparticles. Appl. Phys. Lett. 90 (2007) 133114.
[11] S. Nie, S. R. Emory. Probing Single Molecules and Single Nanoparticles by Surface-Enhanced Raman Scattering. Science 275(1997) 1102-1106
[12] J. –Y. Chu, T. –J. Wang, Y. –C. Chang, M. –W. Lin, J. –T. Yeh, and J. –K.Wang. Multi-wavelength heterodyne-detected scattering-type scanning near-field optical microscopy. Ultramicroscopy 108 (2008) 314-319.
[13] M. Shaban, H. Hamdy, F. Shahin, Joonmo Park, and S.-W. Ryu. Uniform and Reproducible Barrier Layer Removal of Porous Anodic Alumina Membrane. J. Nanosci. Nanotechnol. 10 (2010) 3380-3384.
[14] M. Shaban, M. Ali, K. Abdelhady, A.A. P. Khan, H. Hamdy, Hexagonal arrays of Pt nanocylinders on the top surface of PAA membranes using low vacuum sputter coating technique, Vacuum 161 (2019) 259-267.
[15] M. Shaban, Morphological and Optical Characterization of High Density Au/PAA Nanoarrays, Journal of Spectroscopy 2016 (2016) 8 page [Article ID 5083482].
[16] C. E. Rayford, G. Schatz, and K. Shuford. Optical properties of gold nanospheres. Nanoscape 2 (2005) 27-33.
[17] M. Shaban, H. Hamdy, F. Shahin, and S.-W. Ryu. Strong surface plasmon resonance of ordered gold nanorod array fabricated in porous anodic alumina template. J. Nanosci. Nanotechnol. 10 (2010) 3034-3037.
[18] P.R. Evans, R. Kullock, W. R Hendren, R. Atkinson, R. J.Pollard, and L. M. Eng. Optical Transmission Properties and Electric Field Distribution of Interacting 2D Silver Nanorod Arrays. Adv. Funct. Mater. 18 (2008) 1075 -1079.
[19] N. Felidj, J. Aubard, G. J. Levi, R. Krenn, G. Schider, A. Leitner, and F. R. Aussenegg. Enhanced substrate-induced coupling in two-dimensional gold nanoparticle arrays. Phy. Rev. B 66 (2002) 245407.
[20] T. Atay, J-H. Song, and A. V. Nurmikko Strongly Interacting Plasmon Nanoparticle Pairs: From Dipole−Dipole Interaction to Conductively Coupled Regime. Nano Letters 4 (2004) 1627-1631.
[21] M. Shaban, Ashour M. Ahmed, Ehab M. Abdel Rhman, and Hany Hamdy, "Tunability and Sensing Properties of Plasmonic/1D Photonic Crystal, Scientific Reports 7 (2017) 41983.
[22] M. Rabia., M. Shaban, A. Adel and A.A. Abdel-Khaliek, Effect of plasmonic au nanoparticles on the photoactivity of polyaniline/indium tin oxide electrodes for water splitting. Environmental Progress and Sustainable Energy 38 (2019) 1-8.